Nano Energy 57 (2019) 500–506

Contents lists available at ScienceDirect

Nano Energy

journal homepage: www.elsevier.com/locate/nanoen

Full paper

Surface potential tailoring of PMMA fibers by electrospinning for enhanced triboelectric performance

Tommaso Busolo[a], Daniel P. Ura[b], Sung Kyun Kim[a], Mateusz M. Marzec[c], Andrzej Bernasik[c,d], Urszula Stachewicz[b], Sohini Kar-Narayan[a,*]

[a] Department of Materials Science and Metallurgy, University of Cambridge, CB3 0FS Cambridge, United Kingdom
[b] International Centre of Electron Microscopy for Materials Science, Faculty of Metals Engineering and Industrial Computer Science, AGH University of Science and Technology, A. Mickiewicza 30 Av., 30-059 Kraków, Poland
[c] Academic Centre for Materials and Nanotechnology, AGH University of Science and Technology, A. Mickiewicza 30 Av., 30-059 Kraków, Poland
[d] Faculty of Physics and Applied Computer Science, AGH University of Science and Technology, A. Mickiewicza 30 Av., 30-059 Kraków, Poland

ARTICLE INFO

Keywords:
Triboelectric generator
Electrospinning
Poly(methyl methacrylate)
Surface chemistry
Kelvin probe force microscopy
Energy harvesting

ABSTRACT

Triboelectric generators rely on contact-generated surface charge transfer between materials with different electron affinities to convert mechanical energy into useful electricity. The ability to modify the surface chemistry of polymeric materials can therefore lead to significant enhancement of the triboelectric performance. Poly(methyl methacrylate) (PMMA) is a biocompatible polymer commonly used in medical applications, but its central position on the triboelectric series, which empirically ranks materials according to their electron-donating or electron accepting tendencies, renders it unsuitable for application in triboelectric generators. Here, we show that the surface potential of PMMA fibers produced by electrospinning can be tailored through the polarity of the voltage used during the fabrication process, thereby improving its triboelectric performance, as compared to typically spin-coated PMMA films. The change in surface chemistry of the electrospun PMMA fibers is verified using X-ray photoelectron spectroscopy, and this is directly correlated to the changes in surface potential observed by Kelvin probe force microscopy. We demonstrate the enhancement of triboelectric energy harvesting capability of the electrospun PMMA fibers, suggesting that this surface potential modification approach can be more widely applied to other materials as well, for improved triboelectric performance.

1. Introduction

The development of wearable and implantable medical devices has surged in recent years due to their potential to provide real-time health information and personalized medical care [1–3]. However, the majority of this equipment relies on external power sources like batteries to operate, restricting their application for in vivo situations. Furthermore, these batteries require an invasive and costly surgical procedure to be removed at the end of their operational life [4]. A solution to this issue is biomechanical energy harvesters, which are devices capable of transforming human body energy (i.e. kinetic, chemical and thermal) into electrical power [5,6]. Kinetic energy is one of the most abundant and easily available energy sources, making triboelectric energy harvesters a promising technology, as these are capable of converting mechanical energy to electrical energy [7]. Triboelectric generators operate on the principle of a voltage being developed across two dissimilar materials that are contacted and separated, due to a combined effect of contact electrification and electrostatic induction. This energy harvesting method has relatively high efficiency, simple device configuration and low materials cost [8,9]. A key challenge in this field is improving power output through materials selection and/or geometrical modification. The most effective methods to achieve improved triboelectric performance are increasing surface area and altering the surface chemistry of the material [4]. Higher surface area allows for higher charge transfer density, while tailored surface charge properties improve the charge transfer mechanisms.

Poly(methyl methacrylate) (PMMA) is a widely used polymer composite component in photovoltaics [10], but importantly it is also a biocompatible polymer commonly used in orthopedics and optometry [11,12]. Its rigidity, inertness and in situ polymerization capabilities make it widely used as bone cement and for intraocular lenses. These properties make PMMA an interesting material for implantable triboelectric generators. On the triboelectric series, which lists materials according to their electron-donating (tribo-positive) and electron-

* Corresponding author.
E-mail address: sk568@cam.ac.uk (S. Kar-Narayan).

https://doi.org/10.1016/j.nanoen.2018.12.037
Received 11 October 2018; Received in revised form 1 December 2018; Accepted 10 December 2018
Available online 11 December 2018

accepting (tribo-negative) tendencies, PMMA typically features near the middle of this empirical series. PMMA has been used in triboelectric devices as a tribo-positive material, but its lower degree of tribo-positivity in comparison with more commonly used materials, such as polyamides, has limited its usage in triboelectric generators [13]. However, the PMMA surface can be engineered to improve its triboelectric output as shown by Taghavi et al. [14], although previous studies of electrospun PMMA fibers were not used for any triboelectric performance evaluation [15]. In electrospinning, a high voltage is applied between the nozzle of a syringe filled with a polymer solution and a grounded substrate held at some distance away from the nozzle. A polymer solution jet emerges from the nozzle at a critical voltage, followed by evaporation of the solvent to produce solid fibers on the grounded substrate [16]. Applying a positive or negative voltage to the nozzle generates charges of equivalent polarity at the liquid jet–air interface during the electrospinning process, causing molecular orientation of chemical functional groups of the polymer chains at the surface of fibers [17]. Consequently, electrospinning can be used to effectively tailor the surface chemistry of fibers by alternating voltage polarities in a single-step manufacturing process. Therefore, this fabrication technique has the potential to enhance the triboelectric properties of PMMA by engineering both its surface area (due to the fiber geometry) as well as the surface chemistry (by controlling the polarity of applied voltage during electrospinning).

Here we demonstrate a one-step process using electrospinning to substantially alter the surface chemistry of PMMA fibers and consequently improve their triboelectric output performance. The PMMA fibers were produced using opposite voltage polarities to modify the surface chemistry. The change in surface chemistry was correlated with a shift in spatially resolved surface potential and charge transfer affinity. The variation of the nanoscale surface potential properties was directly related to the distinct enhancement of the triboelectric performance observed in the electrospun PMMA fibers.

2. Results and discussion

PMMA fibers were successfully fabricated using positive (PMMA+) and negative (PMMA−) voltage polarities, as indicated in Fig. 1. The scanning electron microscopy (SEM) images and corresponding fiber diameter histograms revealed similar size distribution for both samples. The average PMMA+ fiber diameter was 1.56 ± 0.2 μm, and the average PMMA− fiber diameter was 1.6 ± 0.24 μm. The morphology of both types of fibers was found to be smooth and uniform across all surfaces, regardless of the applied voltage polarities during electrospinning.

Table 1
XPS results from the grazing angle measurement (10°), expressed as % atomic, for electrospun PMMA fibers produced with positive (PMMA+) and negative (PMMA−) voltage polarities, and spin coated PMMA film.

	C1 [%]	C2 [%]	C3 [%]	C4 [%]	O1 [%]	O2 [%]
PMMA+	27.8	16.1	14.0	15.7	12.1	14.4
PMMA−	34.4	15.4	9.8	14.6	11.6	14.3
PMMA film	31.0	14.8	13.2	14.3	10.9	15.8

The surface chemistry of the electrospun PMMA fibers was analyzed using X-ray photoelectron spectroscopy (XPS). The analysis depth was restricted to 1 − 2 nm as the angle between analyzer and sample surface was set to 10°. Deconvoluted spectra collected for O1s regions for PMMA+ and PMMA− samples (see Supplementary Fig. S2) with the atomic concentrations representing each chemical state are collectively presented in Table 1. C1s spectra can be fitted with four components arising from different chemical states of carbons within the PMMA structure.

From Table 1, it can be noticed that in case of positive voltage polarity applied during electrospinning (PMMA+), more oxygen containing groups were present at the surface (and sub-surface) region, whereas in case of negative voltage polarity (PMMA−), the surface contained more C–C type bonds. The largest variation is seen in O1 as its molecular arrangement is more mobile than O2 (Fig. 1d). Interestingly, a spin-coated PMMA film in comparison showed significantly different O1 and O2 content compared to the electrospun PMMA fibers, confirming that molecular reorientation does occur according to the voltage polarity applied during electrospinning. These results indicated that the position of oxygen in the ester group in relation to the fiber surface can be controlled by the applied voltage polarity during the

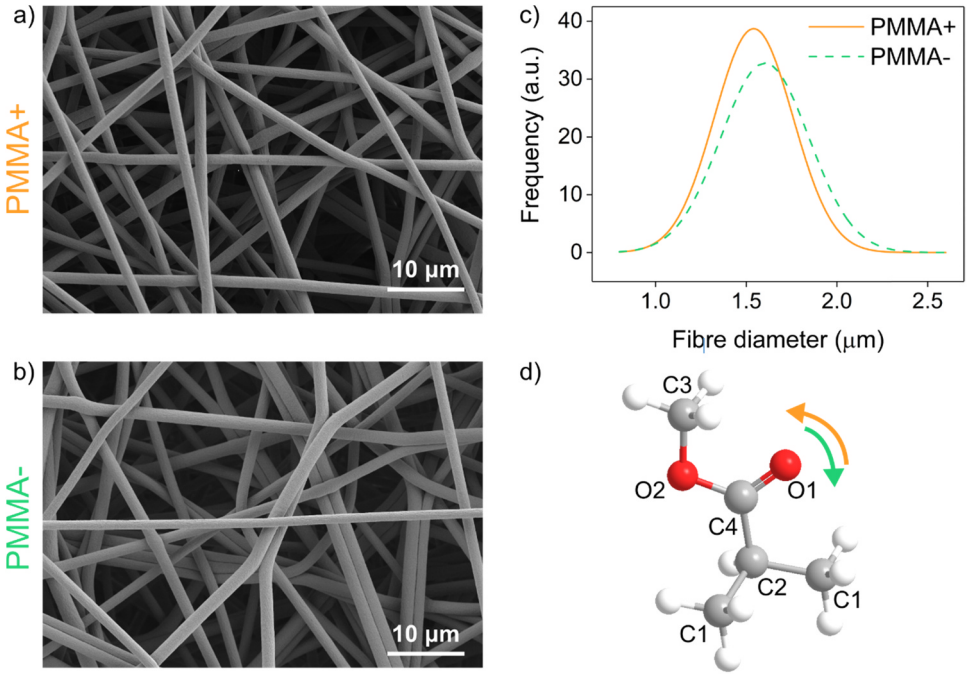

Fig. 1. SEM image of electrospun PMMA fibers produced with a) positive b), negative voltage polarities. c) Fiber average diameter histograms. d) Schematic structure of the single unit of PMMA polymer chain, the atomic label refers to the XPS data shown in Table 1.

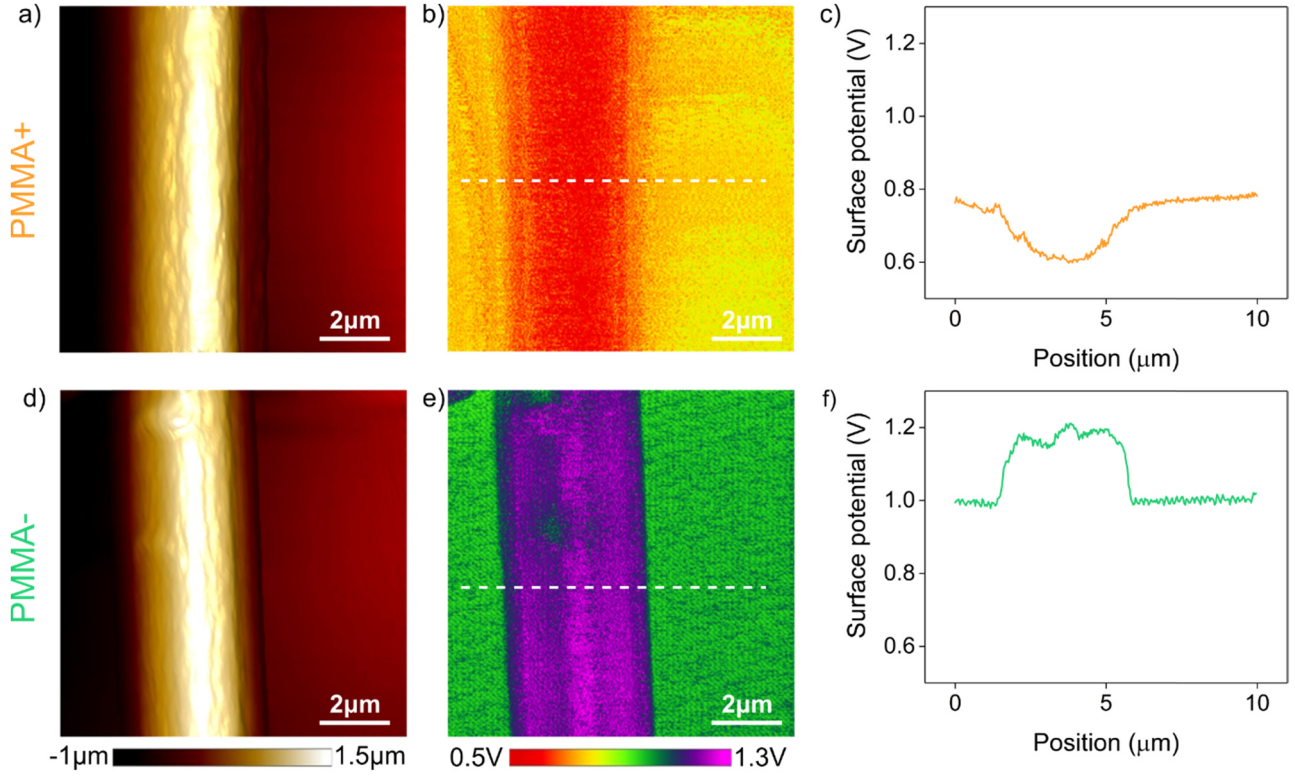

Fig. 2. AFM data of PMMA fibers. a) Topography. b) Surface potential. The dashed line shows the position of the line scan. c) X axis line profile of surface potential of PMMA+. d) Topography. The dashed line shows the position of the line scan. f) X axis line profile of PMMA− fibers.

production of PMMA fibers, as previously shown for other polymers [17–20].

The effect of the tailored surface chemistry on the surface potential of PMMA fibers was investigated using spatially resolved scanning probe techniques, namely atomic force microscopy (AFM) for topographic imaging, and Kelvin probe force microscopy (KPFM) for surface potential imaging. Fig. 2 shows the height and surface potential of various electrospun PMMA fibers on Au coated Si substrate. Although the two PMMA fiber types had similar topography, their surface potential showed a distinct difference. In the case of PMMA+, the surface potential of the fiber had an approximate value of 0.6 V. On the other hand, the surface potential of the PMMA− fiber was approximately 1.2 V.

The difference in surface potential was directly correlated with the shift in surface chemistry displayed in the XPS data. PMMA+ fibers exhibited a lower surface potential due to the higher content of oxygen on their surface compared to PMMA− fibers. Fewer methyl groups were also present on the PMMA+ fibers surface, but the high electronegativity of oxygen is the main contributor to the reduction in surface potential observed. The surface potential of the electrospun PMMA film was found to be 1.05 V, which was in between the surface potential values of the two types of electrospun PMMA fibers, see Supplementary Fig. S4. This is in agreement with different oxygen content (O1 and O2) on the surface between the film and the fibers.

To verify the effect of tailored surface potential on the surface charge transfer affinity, we performed localized triboelectric experiments using a cobalt–chromium (CoCr) coated Si AFM tip. The surface charge transfer properties of the PMMA fibers were investigated in the AFM setup, by rubbing the sample surface with the tip in contact-mode AFM, as shown in Fig. 3. Immediately after the rubbing, the surface potential was measured using KPFM and compared with the initial KPFM data prior to rubbing shown in Fig. 2. It was observed that the surface potential of the rubbed region significantly dropped in both fiber types. The surface potential of the rubbed PMMA+ and PMMA− were −1.2 and 0.1 V, respectively. The surface potential of rubbed spin-coated PMMA film was −1.09 V in comparison, which was again in between the surface potential values of the rubbed PMMA fibers (see Supplementary Fig. S5).

The reduction in surface potential was due to the transfer of charges from the AFM tip to the fiber surface during the rubbing process, indicating a higher position of the tip on the triboelectric series relative to both types of PMMA fibers. Interestingly, the KPFM data from the rubbing tests showed that upon contact, PMMA+ fibers a higher tendency to accept charges than PMMA− fibers, thus indicating that the surface of the former was more electronegative. This was again related to the higher oxygen content present on the surface of PMMA+ fibers, as confirmed by XPS, and as reflected in the initial KPFM data shown in Fig. 2. The charge transfer affinity measured with this experiment has been shown to be related to the work function of the material and therefore its position on the triboelectric series [21]. This suggests that the position of the PMMA on the triboelectric series could be effectively tuned by the manufacturing method. In particular, electrospinning while applying positive voltage polarities results in PMMA fibers that are lower down in the triboelectric series, whereas negative applied voltage during electrospinning resulted in PMMA fibers that were more tribo-positive. In comparison, the data shows that the position of spin-coated PMMA film (with no applied voltage) on the triboelectric series was in between those of the respective electrospun PMMA fibers.

The triboelectric performance of the two types of PMMA fibers was investigated by fabricating triboelectric generators based on these. The fibers were deposited onto an aluminium foil and periodically impacted with a copper substrate that served as the counter-electrode, as shown in Fig. 4f. The fibers were tested with a cyclic force of ~0.7 N at a frequency of 2 Hz using a bespoke measurement setup that has been previously described [22,23].

The open-circuit voltage (V_{oc}) and short-circuit current (I_{sc}) of the PMMA− fiber based triboelectric generator were measured as benchmarks for triboelectric output (see Supplementary Fig. S6). Under

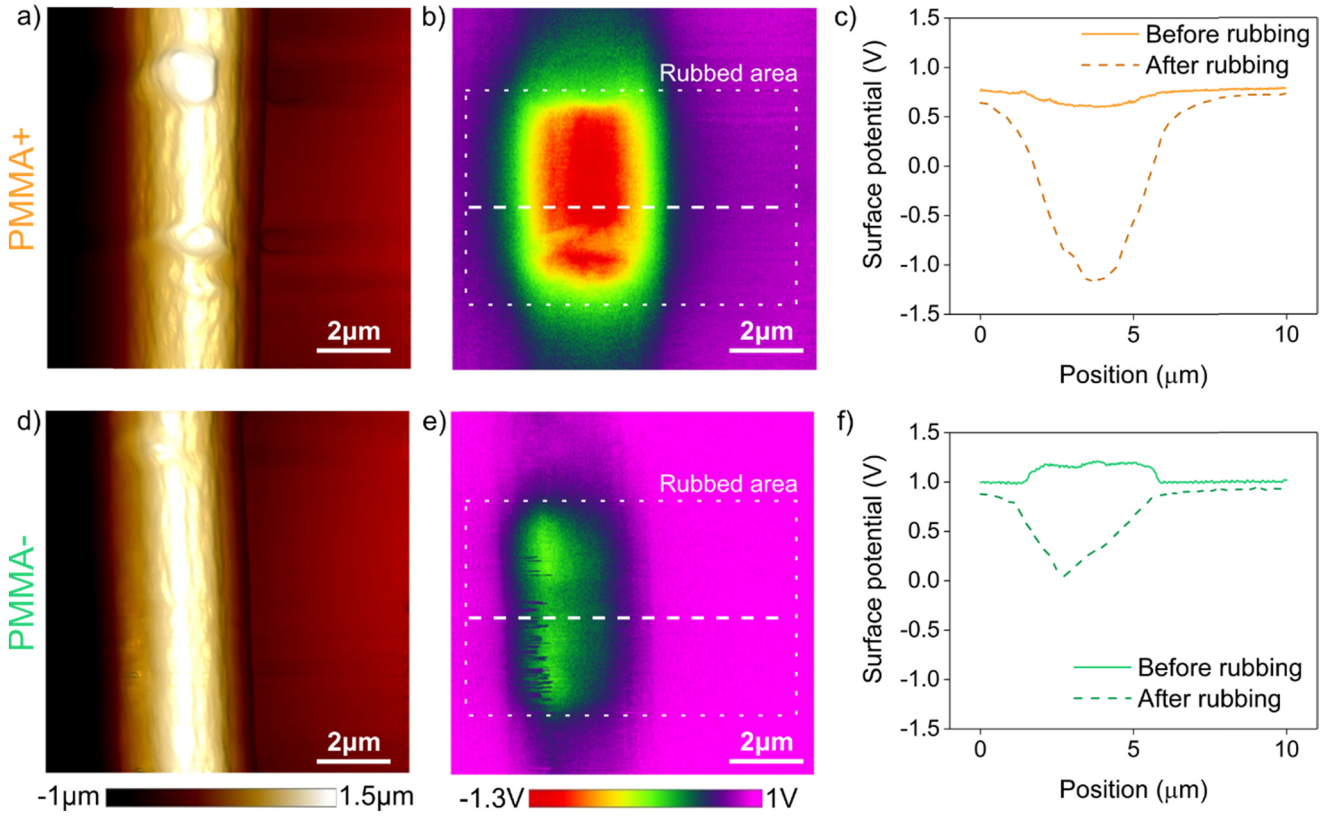

Fig. 3. AFM data of PMMA fibers after rubbing. a) Topography. b) Surface potential. The dotted rectangle indicates the rubbed area. The dashed line shows the position of the line scan. c) X axis line profile of surface potential of PMMA+. d) Topography. e) Surface potential. The dotted rectangle indicates the rubbed area. The dashed line shows the position of the line scan. f) X axis line profile of PMMA− fibers.

identical mechanical excitation, and for identical device geometries, the PMMA+ and PMMA− generators produced a peak V_{oc} of 2.9 and 5.7 V, respectively. The peak I_{sc} of these samples were found to be 67.7 and 148.7 nA, respectively. To further evaluate the power generation potential of the electrospun PMMA fibers, the root mean squared (RMS) voltage and current of the triboelectric generators were measured

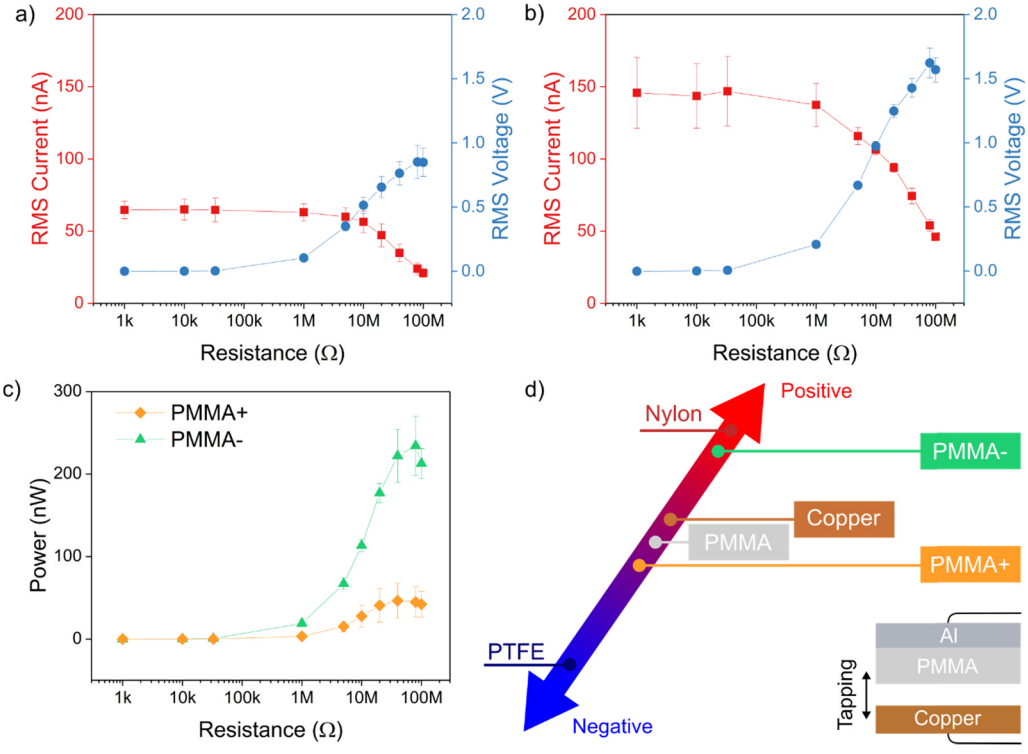

Fig. 4. Triboelectric performance of electrospun PMMA fibers. a) RMS voltage and current of PMMA+ across several load resistances. b) RMS voltage and current of PMMA− across several load resistances. c) Power output of PMMA+ and PMMA− triboelectric generators. d) Schematic of the effect of the surface charge tailoring process on the position of PMMA fibers on the triboelectric series.

across several external load resistances, as shown in Fig. 4. The RMS value was representative of the equivalent steady DC voltage and current that the triboelectric generators can supply to a device. Fig. 4a and b show that the PMMA− based triboelectric generator had higher RMS voltage and current than that of PMMA+ based triboelectric generator across all load resistances measured. The average power output of the two triboelectric generators is plotted in Fig. 4c. The PMMA− triboelectric generator had a maximum average power output of 234.4 nW at a load resistance of 80 MΩ, whereas the PMMA+ triboelectric generator had a maximum average output of 46.6 nW at 40 MΩ, under the testing conditions used. The PMMA− device therefore produced a maximum output power that was five times higher than that of the PMMA+ device. The power output of a triboelectric generator based on spin-coated PMMA film was found to be significantly lower in comparison to the electrospun fibers (see Supplementary Fig. S7).

The clear difference observed in the triboelectric generator performance between the two types of electrospun PMMA fibers was clearly related to the change in surface chemistry induced by the fabrication process. The triboelectric output is empirically related to the position of the two materials on the triboelectric series, while the position of a material is related to its surface potential. A high surface potential material tends to donate charge (tribo-positive), whereas a low surface potential material prefers to gain charge (tribo-negative). In practical terms, the larger the difference in surface potential between the materials, the higher the triboelectric performance of the corresponding generator. PMMA is marginally more positive on the triboelectric series than copper [13], and therefore triboelectric generators comprising spin-coated PMMA films with no surface modification and copper, showed almost negligible power output in response to the mechanical excitation used here. However, electrospinning PMMA was found to permanently modify the surface potential of PMMA, shifting its position on the series. The long-term stability of the surface modification for both types of PMMA fibers was demonstrated by fatigue testing (see Supplementary Fig. S8), with the PMMA− fibers showing more reliable fatigue performance than the PMMA+ fibers.

The PMMA− fiber surface had a lower oxygen content which was correlated with an increase in surface potential. On the contrary, the PMMA+ fibers show a higher oxygen content on the surface and thus a lower surface potential. This indicates that the applied voltage in the electrospinning process caused the PMMA− fibers to be more tribo-negative, while using the opposite polarity caused the PMMA+ fiber to be more tribo-positive. Fig. 4d indicates how the shift in surface chemistry is related to the position of PMMA in the triboelectric series, and how this affects the triboelectric performance. PMMA+ fibers had the larger surface potential difference with respect to copper and therefore had the highest triboelectric output. This argument is further supported by the nature of the I_{sc} curves shown in Supplementary Fig. S6. Triboelectric generators based on both PMMA+ fibers and spin-coated PMMA films showed a positive output during pressing and a negative output during releasing. On the other hand, the triboelectric generator based on PMMA− fibers exhibited the opposite output polarity upon press and release. The difference in the triboelectric performance observed between the two types of electrospun fibers can be attributed to the surface chemistry tailoring process, rather than to differences in surface morphology, as both have been shown to have nominally identical surface morphologies in Figs. 1 and 2. The results were found to be consistent and reproducible across several devices that were tested.

3. Conclusions

In this work, we have demonstrated the surface potential modification of PMMA fibers produced by electrospinning, resulting from changing the polarity of the voltage applied to the nozzle during the fabrication process. We showed, using XPS data from the surfaces of the electrospun PMMA fibers, that in the case of positive voltage polarity applied during electrospinning (PMMA+), more oxygen containing groups were present at the surface (and sub-surface) region, than in the case of negative voltage polarity (PMMA−). A typical spin-coated PMMA film showed significantly different O1 and O2 content compared to the electrospun PMMA fibers, confirming that molecular reorientation does occur according to the voltage polarity applied during electrospinning. The modified surface chemistry of the electrospun PMMA fibers resulted in differences in surface potential as observed by KPFM, indicating that PMMA+ fibers adopted a more tribo-negative character, while PMMA− adopted a much higher tribo-positive character. The implication of this on the triboelectric performance was tested measuring the electrical output of triboelectric generators based on these fibers, where the counter-electrode was chosen to be copper. We found that devices based on both PMMA+ and PMMA− fibers significantly outperformed PMMA film-based triboelectric generators, with PMMA− fibers producing the highest power output under the same mechanical testing conditions. We therefore conclude that controlling the polarity of the voltage applied during electrospinning can be used as an effective method to tailor the surface chemistry of polymeric materials, giving rise to a significant improvement in their triboelectric performance. In this way, biocompatible materials, such as PMMA, which are not ordinarily suitable for triboelectric generators, can be made to have enhanced triboelectric properties, possibly for in vivo energy harvesting applications.

4. Methods

4.1. Materials

Polymethyl methacrylate (PMMA, M_w = 350,000 g mol^{-1}) and N,N-dimethylformamide (DMF) were purchased from Sigma Aldrich, UK. Prior to the solution preparation, the polymer was dried at 70 °C for 24 h. The 12 wt% PMMA solution was stirred for 2.5 h at the 55 °C set on the hot plate (IKA RCT basic, Germany).

4.2. Electrospinning

Electrospinning of PMMA was achieved using apparatus EC-DIG with climate chamber system (IME Technologies, the Netherlands) at the temperature of 25 °C and humidity 40%, (see Supplementary Fig. S1). A positive and negative voltage polarities of 12 kV were applied between the needle and counter electrode covered with an aluminium sheet, keeping the distance between them at 15 cm. The flow rate for the polymer solution was 4 ml h^{-1}. For XPS and KPFM the PMMA fibers were deposited on Au coated Si wafers.

4.3. Spin-coating

PMMA films from were spin-coated (L2001A v.3, Ossila, UK) at the rotation speed of 2500 rpm for 20 s after placing 0.1 mL of the same PMMA solution used for electrospinning on the aluminium foil attached to glass slides.

4.4. Scanning electron microscopy

PMMA fibers were imaged using Scanning Electron Microscope (SEM, Merlin Gemini II, ZEISS, Germany). Fiber diameters (D_f) were analyzed from SEM images using ImageJ (v.1.51g, USA) to produce histograms based on 100 measurements.

4.5. XPS

XPS analysis were taken using PHI VersaProbeII apparatus (ULVAC-PHI, Chigasaki, Japan) equipped with monochromatic Al K_α (1486.8 eV) X-ray source focused to 25 μm spot. The hemispherical analyzer with pass energy set to 23.50 eV was used to determine the

kinetic energy of emitted photoelectrons. The photoelectron take-off angle, defined as an angle between sample surface and analyzer, was set to 10° which limits the depth of analysis to 1 ÷ 2 nm. Charge neutralization was done by irradiating the surface with 1 eV electrons and 7 eV Ar^+ ions. Spectra have been charge corrected to the main line of the carbon C 1s spectrum set to 284.8 eV. Spectra deconvolution and further analysis were performed using PHI Multipak (v 9.8.0.19) software.

4.6. KPFM

The AFM-based measurements were performed using a commercial system (Multi mode 8, Bruker). The surface potential and triboelectric properties of PMMA film and fiber (diameter ≈ 3 μm) were measured via Kelvin probe force microscopy (KPFM), see Fig. S4d. We used the conducting AFM cantilever (MESP-RC-V2, Bruker) with a spring constant of 5 N/m, a resonance frequency of 150 kHz and Cobalt–Chromium (CoCr) coated Si tip. For the KPFM measurements, a 2 V AC signal with a frequency of 20 kHz was applied to the sample by the inter lock-in amplifier in non-contact mode.

The surface potential was determined at the highest point of the fiber as it is the location with minimal height induced error. The samples for KPFM analysis were prepared by direct deposition of PMMA fibers on the Au coated silicon wafers. The substrates were placed in the applied electric field therefore a minimal shift in surface potential in Au coating is expected. AFM analysis was performed on PMMA fibers of similar diameter to minimize the measurement error caused by the size difference. The surface potential of the gold substrate was measured for calibration, see Fig. S4.

4.7. Electrical output characterization

The electrical output performance of triboelectric generators was measured using a bespoke energy harvesting measurement setup [22,23]. The output voltage and current were recorded via a multimeter (Keithley 2002) and a picoammeter (Keithley 6487), respectively. A copper electrode was used to cyclic tap the PMMA sample. The applied force was ~0.7 N at 2 Hz frequency. The low testing force and frequency were purposely selected to simulate realistic human body operating conditions The contact area was 676 mm^2. All samples have comparable thickness to minimize measurement variation. The measurements were recorded after 30 min of tapping in order to stabilize the electrical output. Three devices of each PMMA fiber type and film were tested.

Acknowledgments

S.K.-N. is grateful for financial support from the European Research Council through an ERC Starting Grant (Grant no. ERC-2014-STG-639526, NANOGEN). T.B acknowledges funding from the EPSRC Cambridge NanoDTC, EP/G037221/1. U.S. thanks National Science Centre in Poland for the Uwertura 1 grant, No 2017/24/U/ST5/00397 and Sonata Bis 5 project, No 2015/18/E/ST5/00230 allowing PMMA study and PhD scholarship for D.P.U. Supporting data for this paper is available at the DSpace@Cambridge data repository (https://doi.org/10.17863/CAM.34315).

Appendix A. Supporting information

Supplementary data associated with this article can be found in the online version at doi:10.1016/j.nanoen.2018.12.037.

References

[1] S. Park, S. Jayaraman, Enhancing the quality of life through wearable technology, IEEE Eng. Med. Biol. Mag. 22 (2003) 41–48, https://doi.org/10.1109/MEMB.2003.1213625.
[2] L. Piwek, D.A. Ellis, S. Andrews, A. Joinson, The rise of consumer health wearables: promises and barriers, PLoS Med. 13 (2016) 1–9, https://doi.org/10.1371/journal.pmed.1001953.
[3] A. Tricoli, N. Nasiri, S. De, Wearable and miniaturized sensor technologies for personalized and preventive medicine, Adv. Funct. Mater. 27 (2017) 1–19, https://doi.org/10.1002/adfm.201605271.
[4] Z.L. Wang, J. Chen, L. Lin, Progress in triboelectric nanogenerators as a new energy technology and self-powered sensors, Energy Environ. Sci. 8 (2015) 2250–2282, https://doi.org/10.1039/c5ee01532d.
[5] Y.M. Choi, M.G. Lee, Y. Jeon, Wearable biomechanical energy harvesting technologies, Energies 10 (2017), https://doi.org/10.3390/en10101483.
[6] A. Proto, M. Penhaker, S. Conforto, M. Schmid, Nanogenerators for human body energy harvesting, Trends Biotechnol. 35 (2017) 610–624, https://doi.org/10.1016/j.tibtech.2017.04.005.
[7] C. Dagdeviren, Z. Li, Z.L. Wang, Energy harvesting from the animal/human body for self-powered electronics, Annu. Rev. Biomed. Eng. 19 (2017) 85–108, https://doi.org/10.1146/annurev-bioeng-071516-044517.
[8] Q. Jing, S. Kar-Narayan, Nanostructured polymer-based piezoelectric and triboelectric materials and devices for energy harvesting applications, J. Phys. D Appl. Phys. (2018).
[9] N. Kaur, K. Pal, A comprehensive review on triboelectric nanogenerator as a mechanical energy harvester, Energy Technol. (2017), https://doi.org/10.1002/ente.201700639.
[10] H. Yang, M. Huang, J. Wu, Z. Lan, S. Hao, J. Lin, The polymer gel electrolyte based on poly(methyl methacrylate) and its application in quasi-solid-state dye-sensitized solar cells, Mater. Chem. Phys. 110 (2008) 38–42, https://doi.org/10.1016/j.matchemphys.2008.01.010.
[11] K.C. Glasgow, D. Dhara, An overview of the biocompatability of polymeric, Surf. Polym. Biomed. Appl. (2008) 268–282.
[12] M.F. Maitz, Applications of synthetic polymers in clinical medicine, Biosurf. Biotribol. 1 (2015) 161–176, https://doi.org/10.1016/j.bsbt.2015.08.002.
[13] Y. Zi, Z.S. Wang, L. Lin, C.J. Niu. Triboelectric Nanogenerators. 2016.
[14] M. Taghavi, C. Filippeschi, B. Mazzolai, L. Beccai. Hierarchical surface patterning for triboelectric nanogenerators and sensors, IEEE-NANO, in: Proceedings of the 15th International Conference Nanotechnol, 2015, pp. 1147–1150. ⟨https://doi.org/10.1109/NANO.2015.7388827⟩.
[15] S. Piperno, L. Lozzi, R. Rastelli, M. Passacantando, S. Santucci, PMMA nanofibers production by electrospinning, Appl. Surf. Sci. 252 (2006) 5583–5586, https://doi.org/10.1016/j.apsusc.2005.12.142.
[16] U. Stachewicz, F. Hang, A.H. Barber, Adhesion anisotropy between contacting electrospun fibers, Langmuir 30 (2014) 6819–6825, https://doi.org/10.1021/la5004337.
[17] U. Stachewicz, C.A. Stone, C.R. Willis, A.H. Barber, Charge assisted tailoring of chemical functionality at electrospun nanofiber surfaces, J. Mater. Chem. 22 (2012) 22935–22941, https://doi.org/10.1039/c2jm33807f.
[18] H.W. Tong, M. Wang, Electrospinning of fibrous polymer scaffolds using positive voltage or negative voltage: a comparative study, Biomed. Mater. 5 (2010), https://doi.org/10.1088/1748-6041/5/5/054110.
[19] Q. Zhao, W.W. Lu, M. Wang, Modulating the release of vascular endothelial growth factor by negative-voltage emulsion electrospinning for improved vascular regeneration, Mater. Lett. 193 (2017) 1–4, https://doi.org/10.1016/j.matlet.2017.01.058.
[20] X.Y. Sun, R. Shankar, H.G. Börner, T.K. Ghosh, R.J. Spontak, Field-driven biofunctionalization of polymer fiber surfaces during electrospinning, Adv. Mater. 19 (2007) 87–91, https://doi.org/10.1002/adma.200601345.
[21] K.Y. Lee, S.K. Kim, J.H. Lee, D. Seol, M.K. Gupta, Y. Kim, S.W. Kim, Controllable charge transfer by ferroelectric polarization mediated triboelectricity, Adv. Funct. Mater. 26 (2016) 3067–3073, https://doi.org/10.1002/adfm.201505088.
[22] Y.S. Choi, Q. Jing, A. Datta, C. Boughey, S. Kar-Narayan, A triboelectric generator based on self-poled Nylon-11 nanowires fabricated by gas-flow assisted template wetting, Energy Environ. Sci. 10 (2017) 2180–2189, https://doi.org/10.1039/C7EE01292F.
[23] R.A. Whiter, V. Narayan, S. Kar-Narayan, A scalable nanogenerator based on self-poled piezoelectric polymer nanowires with high energy conversion efficiency, Adv. Energy Mater. 4 (2014) 1–7, https://doi.org/10.1002/aenm.201400519.

Tommaso Busolo is a Ph.D. student in the Department of Materials Science and Metallurgy at the University of Cambridge. He received a MEng degree in materials science from the University of Manchester and an MRes degree in Nanotechnology from the University of Cambridge. His current research is focused on smart textiles for energy harvesting and sensing applications.

Daniel P. Ura is currently a Ph.D. candidate under the supervision of Dr. Urszula Stachewicz at AGH University of Science and Technology and International Centre of Electron Microscopy for Materials Science in Krakow, Poland. He obtained M.Eng in 2017 in materials science. His research is focused on mechanical and surface properties of electrospun polymer fibers.

Dr. Sungkyun Kim works as a postdoctoral researcher with Dr. Sohini Kar-Narayan at University of Cambridge, United Kingdom. He earned the Ph.D. degrees from Advanced Materials Science & Engineering from Sungkyunkwan University, South Korea in 2017. His research interests include atomic force microscopy studies of piezoelectric, triboelectric and ferroelectric materials and characterization of 2-D materials and polymer based electromechanical energy harvester.

Mateusz Marzec is an Assistant Professor at Academic Centre for Materials and Nanotechnology, AGH University of Science and Technology in Krakow, Poland. He earned his BSc and MSc degrees in chemistry from Faculty of Fuels and Energy at AGH and his Ph.D. degree in physics from Faculty of Physics and Applied Computer Science, AGH. His current interests are focused on polymer-metal and polymer-polymer interfaces and interfacial engineering in thin film organic-based electronic devices.

Andrzej Bernasik received his M.S., Ph.D. and Habilitation at AGH University of Science and Technology (Kraków, Poland). His main field of interest is physicochemical properties of materials surface and interfaces. In experimental work, he uses mainly methods such as XPS, SIMS and AFM. He gained scientific experience at the Freie Universität (Berlin, Germany) and Ecole des Mines de Nancy (Nancy, France). His current interests are focused on the organic-organic and organic-metal interfaces for optimization of organic electronic devices and biosensors.

Urszula Stachewicz is currently an associate professor at AGH University of Science and Technology in Krakow, Poland, where she obtained her Habilitation (DSc) in 2017. She graduated from Delft University of Technology with Ph.D. in electrohydrodynamic processes and conducted her postdoctoral study at Queen Mary, University of London while working at spin-out company Nanoforce Technology Ltd, UK. Her research is focused on electrospun polymer fibers for tissue engineering and for energy and water harvesting. Her interest is in correlative and advanced microscopy and in situ mechanical testing of synthetic and naturally structured materials.

Sohini Kar-Narayan is a Reader (Associate Professor) in Device & Energy Materials at the Department of Materials Science & Metallurgy at the University of Cambridge. She previously held a Royal Society Dorothy Hodgkin Fellowship in the same department. She received a BSc in Physics in 2001 from the University of Calcutta, India, and MS and PhD in Physics from the Indian Institute of Science, Bangalore. She was the recipient of a World Economic Forum Young Scientist Award in 2015. Her research interests include functional nanomaterials for energy and sensing applications, printed electronics and advanced scanning probe microscopy techniques.